RHIC SEXTANT TEST – PHYSICS AND PERFORMANCE *

J. Wei, W. Fischer, L. Ahrens, J.M. Brennan, K. Brown, R. Connolly, G. F. Dell,
M. Harrison, J. Kewisch, W. W. MacKay, V. Mane, S. Peggs, F. Pilat, T. Satogata,
M. Tanaka, S. Tepikian, P. Thompson, C. G. Trahern, D. Trbojevic, N. Tsoupas
Brookhaven National Laboratory, Upton, New York 11973, USA

Abstract

This paper presents beam physics and machine performance results of the Relativistic Heavy Ion Collider (RHIC) Sextant and AGS-to-RHIC (AtR) transfer line during the Sextant Test in early 1997. Techniques used to measure both machine properties (difference orbits, dispersion, and beamline optics) and beam parameters (energy, intensity, transverse and longitudinal emittances) are described. Good agreement was achieved between measured and design lattice optics. The gold ion beam quality was shown to approach RHIC design requirements.

1 INTRODUCTION

The Sextant Test, a major test of the full accelerator systems and operational machine properties of a single completed sextant[1, 2] of RHIC, was performed with beams of fully stripped gold ions from December 1996 through February 1997. After being extracted from the AGS, the beam was first delivered to the AtR[3, 4] transfer line, where beam operating conditions from the 1995 AtR Test were rapidly restored. In late January, the superconducting magnets were cooled down to their operating temperature of 4.2 K in about 2 days and were subsequently powered to the injection current. On January 26, the first gold beam was steered through the Lambertson magnet, the injection kicker, and the 400 meters of superconducting magnets to a beam dump at the end of the Sextant. In total, 81 8-hour control-room shifts were devoted to the study of beam quality, machine properties, and accelerator system performance. This paper summarizes the physics results of these Sextant Test shifts.

2 BEAM QUALITY MEASUREMENTS

The main purpose of beam quality measurements was to demonstrate the design beam intensity and emittances. Various instrumentation systems[5, 6] in the AGS, AtR, and Sextant were employed, including beam position monitors (BPM), current transformers, wall current monitors, ionization profile monitors (IPM), and fluorescent screen profile monitors (flags).

2.1 Longitudinal Phase-Space Tomography

Particle motion in longitudinal phase space was reconstructed in the AGS using tomographical algorithms (RADON)[7] from a set of wall current monitor profiles recorded over half a synchrotron period. For the reconstruction, the rf voltage was calibrated by observing the synchronous phase difference as transition was crossed at a known ramp rate. Signal width broadening caused by finite cable bandwidth[8] was taken into account. Fig. 1 shows the phase space diagram at an early stage of the test when bunch coalescing was being tuned up to increase the beam intensity. The coalescing process was quickly improved to achieve an intensity of 4×10^8 ions per bunch with a 95% area of 0.5 ± 0.1 eV·s/u (Table 1).

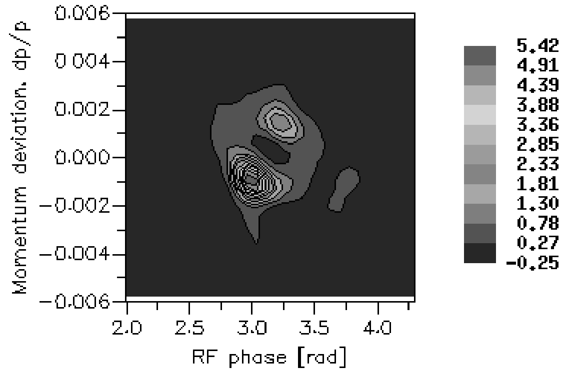

Figure 1: Longitudinal phase space diagram of a Au^{77+} beam in the AGS reconstructed with RADON showing imperfect bunch coalescing at an early stage of the test.

2.2 Transverse Emittances

Transverse beam emittances were measured (Table 1) in the AGS with ionization profile monitors located at places of measured β-functions ($\beta_{x,y} = 22$ m) and dispersion ($D_x =$ 2.2 m). The normalized 95% emittances of 10±1 mm·mr in both horizontal and vertical planes were confirmed by several independent self-consistent measurements[4] in the AtR with flag monitors at multiple locations. Choosing the thick flag uf2 at the minimum $\beta_{x,y}$ in the AtR for the final electron stripping minimized the emittance growth to about 0.7 mm·mrad (7%). A novel prototype IPM[9] was also successfully tested in the AtR, showing good agreement with the flag measurements (Fig. 2) of the transverse beam profile.

Table 1: Comparison of design and achieved Au^{79+} beam quality during the Sextant Test.

Quantity	Unit	Design	Achieved
Momentum	GeV/c/u	11.7	11.31±0.1
Intensity, N	10^9	1	0.4
Bunch area, S	eV·s/u	0.2	0.5±0.1
Emittance, $\epsilon_{Nx,y}$	mm·mrad	10	10±1

* Work supported by the U.S. Department of Energy.

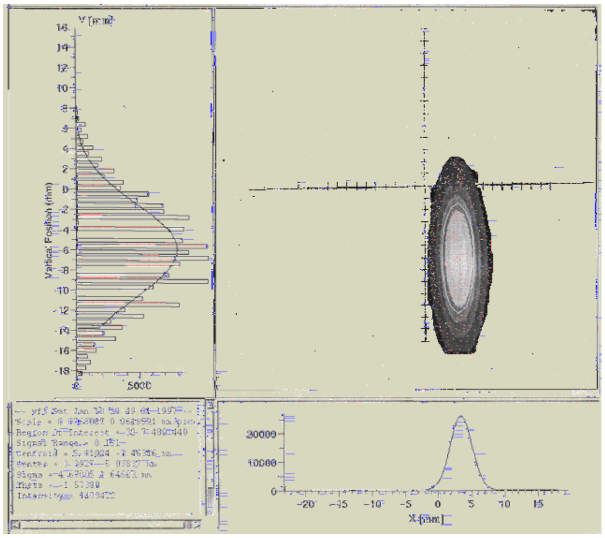

Figure 2: Transverse beam profile in the AtR recorded on flag wf3 (2D image and projections) and IPM (histogram).

2.3 Other Beam Parameters

The beam energy was obtained in the AGS by measuring the magnetic field in the main dipoles with the Gauss clock and a Hall probe. The measured energy with corresponding $\gamma = 12.15 \pm 0.1$ at AGS extraction was confirmed in the AtR by dipole deflection measurements with preset strengths. The beam intensity was consistently measured by several current transformers in the AGS, AtR, and Sextant. Multi-bunch transfer from the AGS to Sextant was also successfully tested and recorded by BPMs and flags.

3 MACHINE LATTICE STUDIES

The primary goals of machine lattice studies were to verify the design optical properties in the AtR and Sextant, and to establish nominal conditions for injection and operations.

3.1 Orbit Correction and Aperture Scan

Due to problems[6, 10] with the BPM system, reference orbits were established in most cases with flags and beam loss monitors, attempting to center the beam on the quadrupoles with three- and four-bump orbit correction schemes. Based on such a partially corrected orbit, Table 2 shows the minimum momentum aperture at critical places of the AGS, AtR, and Sextant. Variation of beam momentum in the AGS (via rf radial loop control) indicated that the momentum acceptance of the AGS extraction septum, the limiting aperture of the entire line, is about $\pm 0.5\%$. The momentum apertures in the AtR and Sextant were deduced from the range of variation in appropriate beamline magnet strengths that did not scrape the beam.

Table 2: Minimum momentum aperture.

Line	Bend	$\Delta p/p$	Comments & Methods
AGS	septum	±0.5%	bumps on, radial loop scan
U	4°, 8°	±1.5%	all ATR magnet scan
W	20°	±0.6%	all ATR magnet PS scan
Y	SWM	±1.7%	switching magnet PS scan
	90°	±1.0%	90° dipole PS scan
	Lamb.	±1.7%	Lambertson PS scan
Sextant	arc	±0.9%	main dipole PS scan

Table 3: Comparison of design and measured lattice optics.

Quantity	Units	Design	Measured
Phase adv./cell		79.2°	78.3° ± 1°
Average β_{max}	m	49.4	49.4±0.1
Average β_{min}	m	10.9	11.2±0.3
Average $D_{x,max}$	m	1.8	2.5±0.4*
Average $D_{y,max}$	m	0	0±0.2*
ξ_x		−4.6	−7*

$*$) Possible systematic error in momentum calibration.

3.2 Transfer Matrices and Difference Orbits

Transfer matrix elements were measured by changing the strength of individual dipole correctors and observing the difference in the downstream orbits. Typical difference orbit excursions in these measurements were ±5 mm. In both horizontal and vertical planes in the AtR, measured orbit differences agreed with those predicted from our lattice model within 1 mm. Due to BPM problems, no reliable difference orbit measurements were made in the Sextant.

3.3 Dispersion

The dispersions in the AtR and Sextant was measured by varying the beam momentum in the AGS while recording the beam displacements with BPMs and flags. The measured dispersions ($D_{x,y}$) at locations of maximum horizontal dispersion (D_x) in the Sextant is shown in Table 3. Compared with the design value, the relatively large measured dispersion is possibly caused by a systematic error in the calibration of beam momentum at AGS extraction.

3.4 Lattice Optics

The phase advance per cell of the Sextant was measured by varying the strength of a sequence of arc dipole correctors by a fixed amount (1 A) while observing the beam centroid shows the results of measurements made with

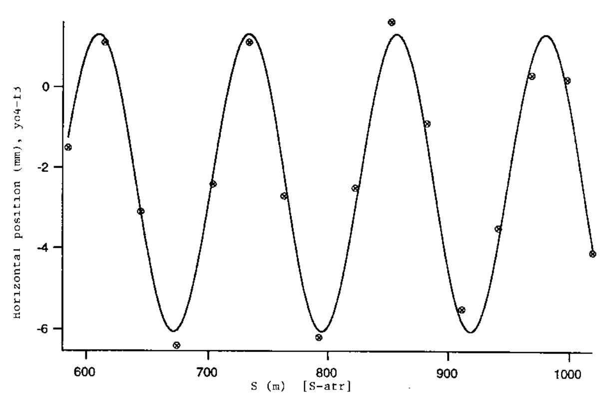

Figure 3: Beam position on the last flag versus perturbation location for Sextant phase advance measurement. The solid line is a sine-wave fit to the data.

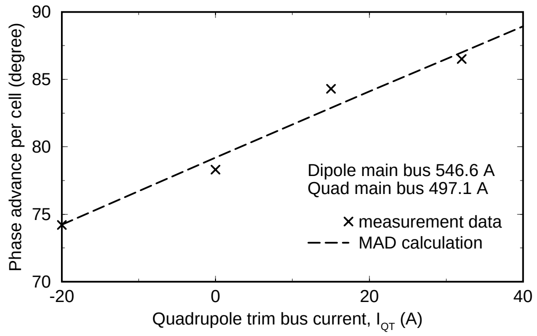

Figure 4: Comparison between the measurement and MAD lattice modeling on horizontal phase advance per cell as a function of arc focusing quadrupole strength.

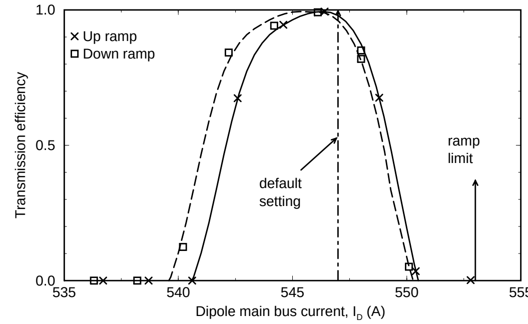

Figure 5: Sextant dipole and quadrupole hysteresis measurement by transmission efficiency scan.

different[11] focusing quadrupole settings. These agree very well with lattice modeling using test stand measurements of the quadrupole Integral Transfer Function (ITF). The β-functions deduced from the phase advance measurements also agreed well with the modeling (Table 3). Horizontal chromaticity ξ_x contributed by the Sextant was measured by evaluating the change in phase advance upon the change in beam momentum at AGS extraction.

4 SYSTEM PERFORMANCE

The primary interest in beam-based system performance analysis was to study stability and repeatability of both accelerator (power supply, kicker, magnet, etc.) and beam instrumentation systems.

4.1 Magnet Hysteresis

Hysteresis effects were measured for the sextant superconducting dipoles (see Fig. 5) and quadrupoles. Due to initial quench protection precautions, the main bus current was only ramped up to slightly above the injection current (about 560 A). After going through a hysteresis scan, differences of 1.1 A in the dipole current and 2.3 A in the quadrupole current were found to restore the original beam position and transmission efficiency. These results qualitatively agreed with test bench measurements, where magnets were ramped up to full current of 5.5 kA, and differences of 1.8 A and 2.3 A were found for dipoles and quadrupoles, respectively.

At the nominal dipole (547 A) and quadrupole (501 A) current settings derived from test bench ITF measurements, a 100% transmission efficiency was observed (Fig. 5). The range of transmission further indicated that the ITF of the arc dipoles (Fig. 5), measured with beam, agreed with the test stand measurements within an accuracy of 0.2%.

4.2 Injection and System Stability

The AGS extraction stability was measured in various ways. The intensity variation was typically $1.9 \pm 0.3 \times 10^8$. On the stripping flag uf2 near the entrance of the AtR, the beam position variations were typically 0.3 mm in the horizontal and 0.05 mm in the vertical plane. Variation in transverse beam size was typically 10%. Relative momentum variations were below the measurable level of 10^{-3}.

Beam centroid positions recorded on nearby BPMs and flags were compared to determine the shot-to-shot repeatability of these systems. The flags showed a repeatability of less than 0.1 mm, and BPMs showed a repeatability of less than 1 mm. Effects produced by power supply noise in the AtR and Sextant were below measurable levels.

5 CONCLUSIONS

The Spring 1997 Sextant Test successfully fulfilled its goal of commissioning the full RHIC accelerator systems with beam. Very good agreement was achieved between measured and design phase advances, and other lattice optics parameters. The quality of the gold beam injected into the RHIC was satisfactory, with transverse emittances close to the design, and intensity only a factor of 2.5 below the design requirement. RHIC is on track towards its completion and operation in 1999.

6 ACKNOWLEDGMENTS

We are thankful to the AGS Main Control Room crews and the Controls Group for their support during the test.

7 REFERENCES

[1] J. Wei and M. Harrison, "The RHIC Project – Design, Status, Challenges, and Perspectives", Proc. XVI RCNP Osaka Intern. Sym. Multi-GeV High-Performance Accel., 1997.

[2] S. Peggs, "RHIC Status", these proceedings.

[3] W.W. MacKay, et al., Proc. 5th EPAC, Sitges, 2376 (1996).

[4] T. Satogata, et al., Proc. 5th EPAC, Sitges, 2379 (1996).

[5] D. Trbojevic, et al., "Preparing Accelerator Systems for the RHIC Sextant Commissioning", these proceedings.

[6] F. Pilat, et al., "RHIC Sextant Test – Accelerator Systems and Performance", these proceedings.

[7] V. Mane, et al., "Beam Tomography in Longitudinal Phase Space", these proceedings.

[8] J. Wei, J.M. Brennan, et al., Proc. 1995 Part. Accel. Conf. and Intern. Conf. on High-Energy Accel., Dallas, 3334 (1995).

[9] R. Connolly et al., "A Prototype Ionization Profile Monitor for RHIC", these proceedings.

[10] T. Shea et al., "Performance of the RHIC Injection Line Instrumentation Systems", these proceedings.

[11] N. Tsoupas et al., "Focusing and Matching Properties of the AtR Transfer Line", these proceedings.